

# Solution of Electromagnetic Propagation Problems in Shielded Transmission Lines Using the Eigenmode Projection Technique

Mohamed O. Ashour<sup>1</sup>, Islam A. Eshrah<sup>1</sup>

<sup>1</sup>(Electronics and Electrical Communication Department, Faculty of Engineering, Cairo University, Egypt)

---

## **Abstract:**

An eigenmode projection technique is utilized to solve the problems of the electromagnetic wave propagation in shielded transmission lines. The technique is adopted to solve the problems of infinite length rectangular shaped loaded lines where a fictitious canonical cavity surrounded by perfect electric surface is chosen to enclose the line and the fields inside are expanded in terms of the cavity solenoidal and irrotational eigenmodes where they are considered as a complete set to represent any vector field inside the cavity. The fields in Maxwell's equations inside the enclosed region are then expanded using the cavity eigenmodes. Finally, a set of equations for the eigenmodes are resolved by using the fields expansions in Maxwell's equations of the cavity where mode projections are done. This set of equations are resolved together to get the line dispersion curve and the propagating modes.

**Key Word:** Eigenmodes; Resonance; Transmission Lines; Microstrip Lines; Coplanar Waveguides.

---

Date of Submission: 15-06-2022

Date of Acceptance: 30-06-2022

---

## I. Introduction

One of the early milestones in microwave engineering was the development of waveguide and other transmission lines for the low-loss transmission of power at high frequencies. Early RF and microwave systems relied on waveguides, two-wire lines, and coaxial lines for transmission where the properties of these lines were studied extensively<sup>1,2</sup> and exact mathematical derivations for the different propagating modes of fields, cut off frequencies, propagation constants, attenuation constants, and characteristic impedance were introduced<sup>3,4</sup>. Planar transmission lines in the form of stripline, microstrip lines, coplanar waveguides, and several other types of related geometries were then invented<sup>5</sup>. They have many advantages where they are lightweight, compact, cost effective, and capable of being easily integrated with active circuit devices to form microwave integrated circuits. However, due to the geometries for these lines, their behaviors and analysis are very complicated<sup>6</sup>. Shielded transmission lines in the form of shielded microstrip lines and shielded coplanar waveguides can be considered good models for their open equivalent lines provided that the dimensions of the shield (closing walls) are adjusted to be equal to or greater than about 10 to 20 times the center conductor width<sup>4</sup>.

For the analysis of the shielded structures, the modal expansion concept was widely used<sup>7,8</sup>. Also, it was integrated with some conventional numerical methods such as the finite-difference time-domain method (FDTD)<sup>9</sup>, the finite element method (FEM)<sup>10</sup>, and the integral equations using moment method (MoM)<sup>11</sup> aiming to produce new hybrid methods. Recently, an eigenmode projection technique (EPT) was introduced and used to solve several electromagnetic problems: resonance<sup>12</sup>, waveguide discontinuities<sup>13</sup>, scattering<sup>14</sup>, transient analysis of waveguide probe excitation<sup>15</sup> and electrostatic<sup>16</sup> problems. The focus of this paper is on the solution of the problems of shielded transmission lines using EPT. In Section II, the formulation of the eigenmode expansion method is presented. Section III covers the eigenmode solution of the infinite length rectangular shaped loaded transmission lines.

## II. The Eigenmode Expansion Method

Throughout this section, the eigenmode expansion method is presented starting with expanding the electric and magnetic fields as a series of different eigenmodes then expanding the derivatives of these fields by following a rigorous mathematical framework to reach the Maxwell's equations for these fields as a series of eigenmodes. Finally, the complex differential equations of electric and magnetic fields are shown as a system of linear equations, where the unknowns are the coefficients of the eigenmodes.

### Eigenmode Expansion

According to Slater<sup>17</sup> and later the modification made by Kurokawa<sup>18</sup>, the eigenmode expansion provides a representation for the electric and magnetic fields in an arbitrary-shaped cavity of volume  $V_t$  enclosed by a surface  $S_t$  which is assumed to be partly perfect electric conducting  $S_E$  and partly perfect magnetic conducting  $S_M$  as shown in Figure 1, in terms of the cavity solenoidal and irrotational eigenmodes as

$$\mathbf{E}(\mathbf{r}) = \sum_n a_n \mathbf{E}_n(\mathbf{r}) + \sum_\alpha f_\alpha \mathbf{F}_\alpha(\mathbf{r}), \quad (1)$$

$$\mathbf{H}(\mathbf{r}) = \sum_n b_n \mathbf{H}_n(\mathbf{r}) + \sum_\lambda g_\lambda \mathbf{G}_\lambda(\mathbf{r}). \quad (2)$$

Where  $a_n, b_n, f_\alpha$  and  $g_\lambda$  represent the coefficients of the cavity fields.  $\mathbf{E}_n(\mathbf{r})$  and  $\mathbf{H}_n(\mathbf{r})$  are the solenoidal electric and magnetic eigenmodes, respectively.  $\mathbf{F}_\alpha(\mathbf{r})$  and  $\mathbf{G}_\lambda(\mathbf{r})$  are the irrotational electric and magnetic eigenmodes, respectively. The solenoidal eigenmodes are coupled through the curl equations

$$\nabla \times \mathbf{E}_n(\mathbf{r}) = k_n \mathbf{H}_n(\mathbf{r}), \quad \nabla \times \mathbf{H}_n(\mathbf{r}) = k_n \mathbf{E}_n(\mathbf{r}). \quad (3)$$

and satisfy the homogeneous Helmholtz equation.

$$(\nabla^2 + k_n^2) \mathbf{E}_n(\mathbf{r}) = 0, \quad (\nabla^2 + k_n^2) \mathbf{H}_n(\mathbf{r}) = 0. \quad (4)$$

The irrotational eigenmodes are represented by the scalar potentials  $(\Phi_\alpha, \Psi_\lambda)$  gradient through

$$l_\alpha \mathbf{F}_\alpha(\mathbf{r}) = \nabla \Phi_\alpha, \quad w_\lambda \mathbf{G}_\lambda(\mathbf{r}) = \nabla \Psi_\lambda. \quad (5)$$

and those scalar potentials satisfy Helmholtz equation.

$$(\nabla^2 + l_\alpha^2) \Phi_\alpha = 0, \quad (\nabla^2 + w_\lambda^2) \Psi_\lambda = 0. \quad (6)$$

where  $k_n, l_\alpha, w_\lambda$  are the wavenumbers for the solenoidal and irrotational electric and magnetic fields, respectively.

The cavity eigenmodes discussed above form a complete orthonormal set. Also, the projections between solenoidal and irrotational modes vanish<sup>19</sup>.

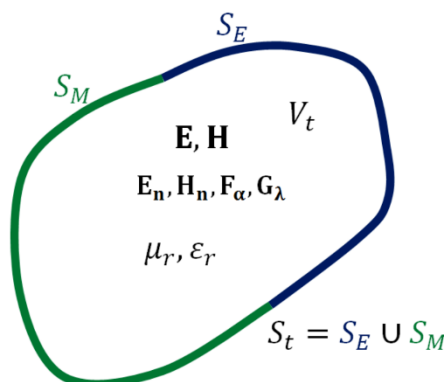


**Figure 1:** An arbitrary-shaped cavity of volume  $V_t$  enclosed by a surface  $S_t$ , and its orthogonal eigen functions.

### Field Derivatives Expansion

The expansions cannot be employed to determine the curl and the divergence terms directly. The curl operator over the electric and magnetic fields can be represented as<sup>18,19,20</sup>

$$\nabla \times \mathbf{E} = \sum_n (k_n a_n + \langle \mathbf{E}, \mathbf{H}_n \rangle_{S_t}) \mathbf{H}_n + \sum_\lambda (\langle \mathbf{E}, \mathbf{G}_\lambda \rangle_{S_t}) \mathbf{G}_\lambda \quad (7)$$

$$\nabla \times \mathbf{H} = \sum_n (k_n b_n + \langle \mathbf{H}, \mathbf{E}_n \rangle_{S_t}) \mathbf{E}_n + \sum_\alpha (\langle \mathbf{H}, \mathbf{F}_\alpha \rangle_{S_t}) \mathbf{F}_\alpha \quad (8)$$

Where  $\langle \mathbf{X}, \mathbf{Y} \rangle_{S_t} = \oint_{S_t} \mathbf{X} \times \mathbf{Y}^* \cdot \hat{\mathbf{n}} ds$ .

### Maxwell's Equations Expansion

By substituting the expansions (2) and (7) into the Maxwell's equation  $\nabla \times \mathbf{E} = -j\omega \mu_0 \mathbf{H}$  and performing eigenmode projection with  $\mathbf{H}_n$  and  $\mathbf{G}_\lambda$  and substituting the expansions (1) and (8) into the Maxwell's equation  $\nabla \times \mathbf{H} = j\omega \epsilon \mathbf{E} + \mathbf{J}$  and performing eigenmode projection with  $\mathbf{E}_n$  and  $\mathbf{F}_\alpha$  using the fact that the modes are orthonormal, yields<sup>18,20</sup>

$$k_n a_n + \langle \mathbf{E}, \mathbf{H}_n \rangle_{S_t} = -j\omega \mu_0 \left( \sum_n b_n' \langle \mu_r \mathbf{H}_n', \mathbf{H}_n \rangle + \sum_\lambda g_\lambda' \langle \mu_r \mathbf{G}_\lambda', \mathbf{H}_n \rangle \right) \quad (9)$$

$$\langle \mathbf{E}, \mathbf{G}_\lambda \rangle_{S_t} = -j\omega \mu_0 \left( \sum_n b_n' \langle \mu_r \mathbf{H}_n', \mathbf{G}_\lambda \rangle + \sum_\lambda g_\lambda' \langle \mu_r \mathbf{G}_\lambda', \mathbf{G}_\lambda \rangle \right) \quad (10)$$

$$k_n b_n + \langle \mathbf{H}, \mathbf{E}_n \rangle_{St} = j\omega\epsilon_o \left( \sum_n a_n' \langle \epsilon_r \mathbf{E}_n', \mathbf{E}_n \rangle + \sum_\alpha f_\alpha' \langle \epsilon_r \mathbf{F}_\alpha', \mathbf{E}_n \rangle \right) + \langle \mathbf{J}, \mathbf{E}_n \rangle \quad (11)$$

$$\langle \mathbf{H}, \mathbf{F}_\alpha \rangle_{St} = j\omega\epsilon_o \left( \sum_n a_n' \langle \epsilon_r \mathbf{E}_n', \mathbf{F}_\alpha \rangle + \sum_\alpha f_\alpha' \langle \epsilon_r \mathbf{F}_\alpha', \mathbf{F}_\alpha \rangle \right) + \langle \mathbf{J}, \mathbf{F}_\alpha \rangle \quad (12)$$

Where  $\langle \mathbf{X}, \mathbf{Y} \rangle = \int_{V_t} \mathbf{X} \cdot \mathbf{Y}^* dv$ . this term  $\langle \mathbf{X}, \mathbf{Y} \rangle$  denote the volumetric projection of the two vector functions  $\mathbf{X}$  and  $\mathbf{Y}$ . By putting equations (9)-(12) in matrix form, we obtain

$$\mathbf{K}\mathbf{a} + \mathbf{Q}^{EH} = -j\omega\mu_o (\mathbf{M}^{HH}\mathbf{b} + \mathbf{M}^{GH}\mathbf{g}) \quad (13)$$

$$\mathbf{Q}^{EG} = -j\omega\mu_o (\mathbf{M}^{HG}\mathbf{b} + \mathbf{M}^{GG}\mathbf{g}) \quad (14)$$

$$\mathbf{K}\mathbf{b} + \mathbf{Q}^{HE} = j\omega\epsilon_o (\mathbf{W}^{EE}\mathbf{a} + \mathbf{W}^{FE}\mathbf{f}) + \mathbf{V}^{JE} \quad (15)$$

$$\mathbf{Q}^{HF} = j\omega\epsilon_o (\mathbf{W}^{EF}\mathbf{a} + \mathbf{W}^{FF}\mathbf{f}) + \mathbf{V}^{JF} \quad (16)$$

where  $\mathbf{K}$  is a diagonal matrix with diagonal elements  $k_n$ ,  $\mathbf{M}_{nn}^{XY} = \langle \mu_r \mathbf{X}_n', \mathbf{Y}_n \rangle$ ,  $\mathbf{W}_{nn}^{XY} = \langle \epsilon_r \mathbf{X}_n', \mathbf{Y}_n \rangle$ ,  $\mathbf{Q}_n^{XY} = \langle \mathbf{X}, \mathbf{Y}_n \rangle_{St}$ , and  $\mathbf{V}_n^{XY} = \langle \mathbf{X}, \mathbf{Y}_n \rangle$ .  $\mathbf{X}$  and  $\mathbf{Y}$  can be  $\mathbf{E}$ ,  $\mathbf{H}$ ,  $\mathbf{F}$ ,  $\mathbf{G}$ , or  $\mathbf{J}$ . The above system of equations (13)-(16) represents the EPT core, where these equations are employed to solve the eigenmode problems for rectangular shaped electromagnetic problems in the next two sections.

### III. Propagation Solution for Shielded Transmission Lines

It's required to evaluate the dispersion relation (the resonance frequencies) and the modes of a closed (shielded) rectangular transmission line loaded with dielectric, and lossy metal. The solution of the source-free wave propagation in a closed-boundary loaded structure is similar to the cavity resonance problem<sup>12,13,14,15,16</sup>. Generally, EPT is used to study the resonance of arbitrary-shaped conducting cavity with arbitrary dielectric loading as shown in Figure 2a. The solution flow is as follows: as depicted in Figure 2b, a canonical cavity surrounded by either perfect electric (PE) or perfect magnetic (PM) or composite PE/PM surface is chosen, the canonical cavity solenoidal and irrotational eigenmodes are then derived analytically where they are considered as a complete set to represent any vector field inside the cavity. The main problem is enclosed within this cavity as shown in Figure 2c. The fields inside the enclosed region are expanded in terms of the derived cavity eigenmodes. The eigenvalue problem is finally formed by using these expansions in Maxwell's equations of the cavity where mode projections are done. It's worth mentioning that all PEC materials found in the problem are replaced with highly conductive material, although practical conductors' loss tangent is frequency dependent, it is assumed that the used conductor has a constant loss tangent with high value over the frequency range of interest, which would be almost identical with the theoretical PEC material at microwave frequencies. It is expected that the eigenvalues (resonance frequencies) in this case will be complex, and the spurious modes will be distinguished upon comparing the real and imaginary parts of the eigenvalue of the resulted modes.

Starting from the system of equations (13)-(16), All the surface integrals (integrals that represent the coupling between the outer modes and the canonical cavity eigenmodes) vanish due to the fact of having zero external fields (this is a closed problem and there is no outer modes). Also, dealing with a source-free medium with constant permeability and making use of the case that the cavity eigenmodes form a complete orthonormal set. The system of equations (13)-(16) can be reduced to

$$\mathbf{K}\mathbf{a} = -j\omega\mu_o \mathbf{b} \quad (17)$$

$$0 = -j\omega\mu_o \mathbf{g} \quad (18)$$

$$\mathbf{K}\mathbf{b} = j\omega\epsilon_o (\mathbf{W}^{EE}\mathbf{a} + \mathbf{W}^{FE}\mathbf{f}) \quad (19)$$

$$0 = j\omega\epsilon_o (\mathbf{W}^{EF}\mathbf{a} + \mathbf{W}^{FF}\mathbf{f}) \quad (20)$$

Solving equations (17)-(20) for the coefficients of the solenoidal electric field eigenmodes.

$$\mathbf{b} = -\frac{\mathbf{K}\mathbf{a}}{j\omega\mu_o} \quad (21)$$

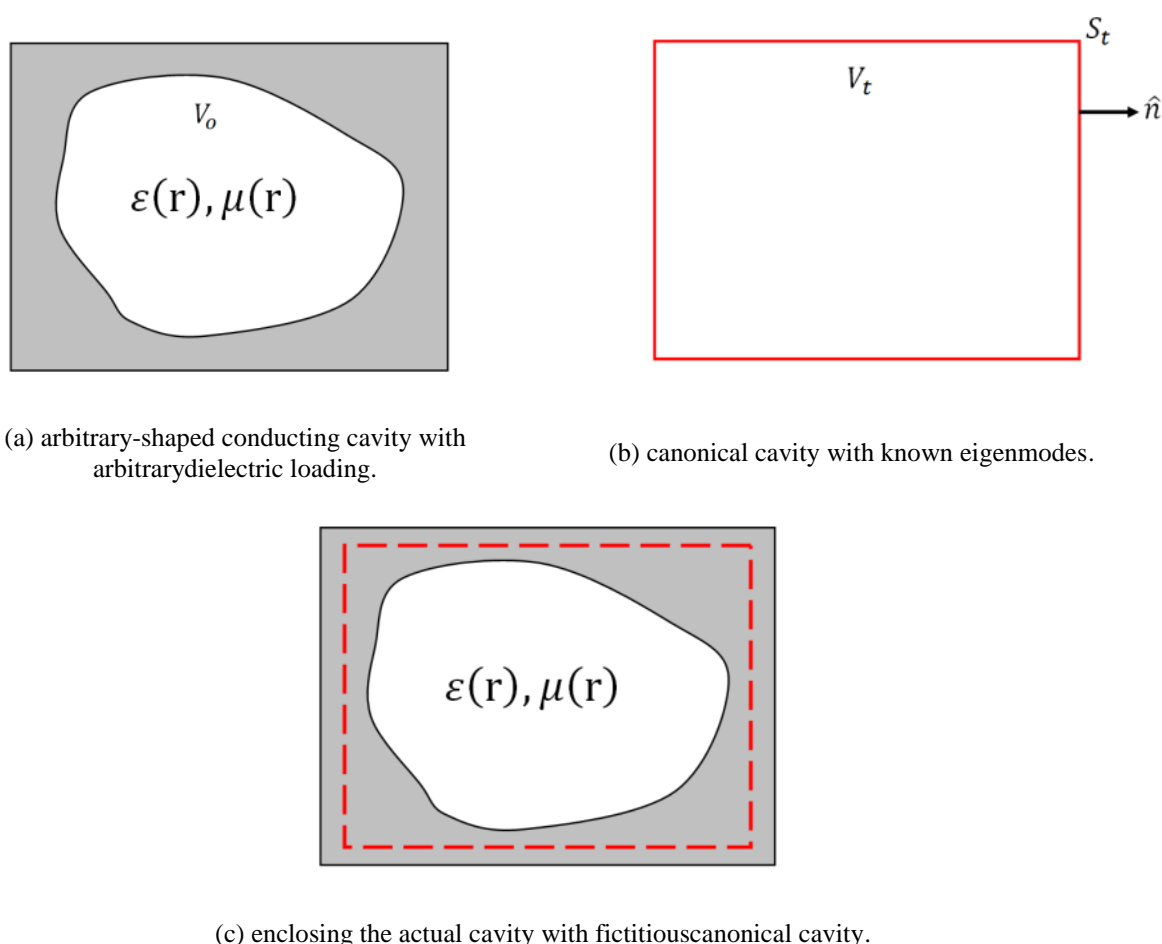


**Figure2:** Model development for the resonance problem using the eigenmode projection technique.

$$\mathbf{f} = -(\mathbf{W}^{FF})^{-1}\mathbf{W}^{EF}\mathbf{a} \tag{22}$$

$$(\mathbf{W}^{EE} - \mathbf{W}^{FE}(\mathbf{W}^{FF})^{-1}\mathbf{W}^{EF})^{-1}\mathbf{K}^2\mathbf{a} - \omega^2\mu_o\epsilon_o\mathbf{a} = 0 \tag{23}$$

Equation (23) can be represented as

$$(\mathbf{\Omega} - k^2\mathbf{I})\mathbf{a} = 0 \tag{24}$$

Where  $k^2 = \omega^2\mu_o\epsilon_o$  and  $\mathbf{I}$  is the identity matrix. So, the dispersion relation can be obtained by computing the matrix eigenvalues where they are used in determining the corresponding wavenumbers. The modal field distribution can be determined by obtaining the eigenvectors  $\mathbf{a}$ . The other solenoidal and irrotational modes can be determined using equations (21),(22).

### Results

First of all, the previous approach is verified for 2 special cases, the canonical case of a PEC rectangular cavity partially filled with dielectric, and the canonical case of a PEC rectangular cavity partially filled with lossy metal. The results of the presented cases are based on the numbering scheme and the modes numbers required for convergence<sup>21</sup> where for any 1D problem, the maximum index used for variations in v direction ( $N_v^{\max}$ ) can be represented as

$$N_v^{\max} = \frac{1}{20\sigma_\epsilon^2} \frac{p}{\Delta_v} \tag{25}$$

Where p is the dimension of an object along the v direction,  $\Delta_v$  is the smallest dimension of an object in the unit cell along the v direction,  $\sigma_\epsilon^2$  is a truncation parameter (to enhance accuracy decrease  $\sigma_\epsilon^2$ ), and the used number of modes is  $N_v^{\max}$ . In general, the numbering scheme of modes used on the following cases is determined by considering all the combinations of different indices representing the mode variations in x and y directions and convergence is achieved by increasing the maximum index used in each direction.

The first case to be considered is a rectangular waveguide partially filled with dielectric material as shown in Figure 3. The waveguide has cross-sectional dimensions  $a = 22.86$  mm,  $b = 10.16$  mm, and the

dielectric has  $d = 5.82$  mm and  $\epsilon_r = 10$ . The dispersion curve obtained using the EPT with the modes numbering scheme shown in Table 1 in comparison with the exact solution for the propagating modes is illustrated in Figure 4. In addition, Figure 5 provides the electric field distribution using the EPT in comparison with the exact one for  $x = a/4$  along the  $y$ -direction. It's to be noted that both figures show excellent agreement with the analytical results for this case<sup>4</sup>.

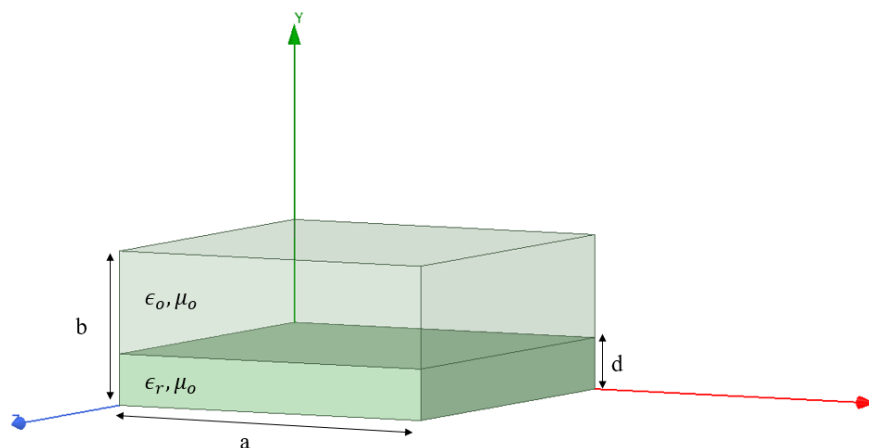


**Figure3:** Rectangular waveguide partially filled with dielectric material.

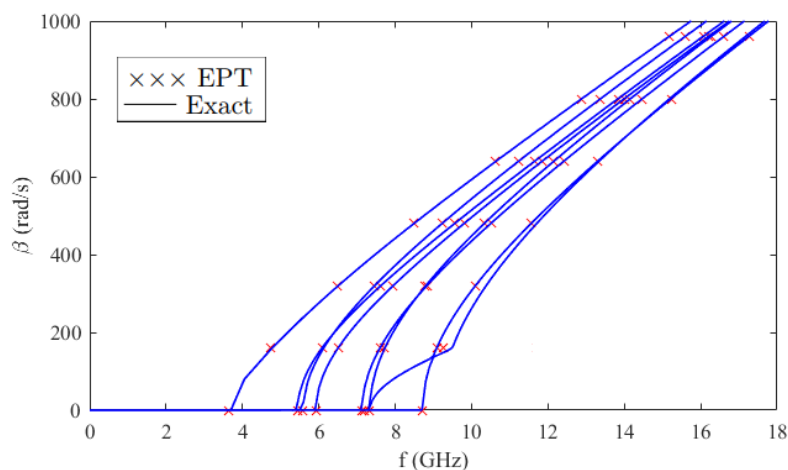


**Figure4:** Dispersion curve of a partially filled waveguide with  $a = 22.86$  mm,  $b = 10.16$  mm,  $d = 5.82$  mm and  $\epsilon_r = 10$ .

The second case to be considered is a rectangular waveguide partially filled with PEC as shown in Figure 6. The waveguide has cross-sectional dimensions  $a = 22.86$  mm,  $b = 10.16$  mm, and the PEC has thickness  $d = 3.38$  mm. For this simple case, the results obtained should be the same as that of an empty waveguide with cross-sectional dimensions  $a \times (b-d)$ . By using the EPT with the modes numbering scheme shown in Table 2, The eigenvalues are complex where they can be separated into two sets: the first set contains the modes resonating in the

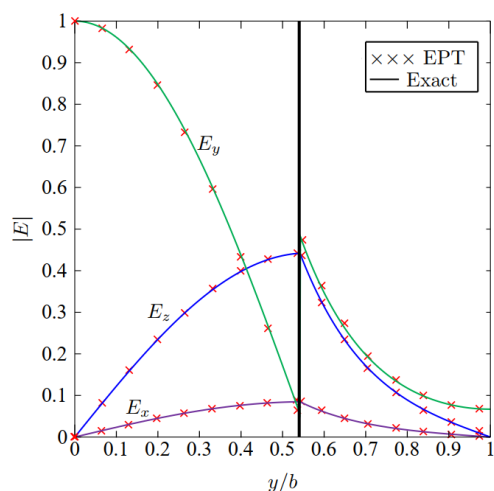


**Figure5:** Electric field distribution for the dominant mode along the y-direction at  $x = a/4$  for a partially filled waveguide with  $a = 22.86$  mm,  $b = 10.16$  mm,  $d = 5.82$  mm and  $\epsilon_r = 10$ .

**Table 1:**Numbering scheme of the modes used to generate results in Figure 4 and Figure 5.

	$n_x$	$n_y$
Solenoidal TE	0,1	j
Solenoidal TM	1	j
Irrotational	1	j
Limits	$0 \leq j \leq 25$	

conductor and the other one contains the modes resonating inside the cavity. The separation of the modes is done by comparing the real and the imaginary parts of the complex cut off wave number. Figure 7 shows the relation between the real part and the imaginary part of the normalized cut off frequency for different loss tangent. The actual modes are the modes with high real part compared to the imaginary part for a  $\tan\delta$  with large value ( $\tan\delta > 10^3$ )<sup>16</sup>. The dispersion curve obtained using the EPT in comparison with the exact solution for the propagating modes is illustrated in Figure 8. In addition, Figure 9 provides the electric field distribution using the EPT in comparison with the exact one. Both figures show excellent agreement with the exact results.

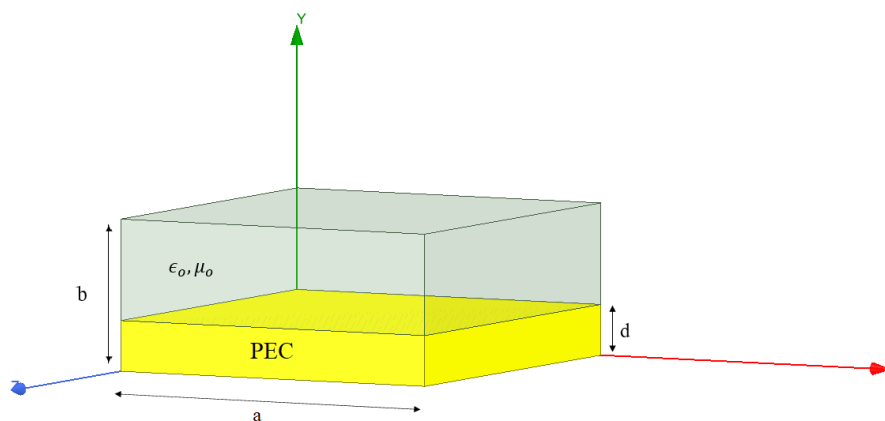


**Figure6:** Rectangular waveguide partially filled with PEC.

Second, shielded microstrip transmission line is a member of the family of the planar microwave transmission lines where it is similar to the basic microstrip line except for the enclosure and the side walls. The metallic enclosure will cover the entire structure as shown in Figure 10. The case to be considered is of a line which has cross-sectional dimensions  $A = 12.7$  mm and  $B = 12.7$  mm, The patch has cross-sectional dimensions  $a = 1.27$  mm and  $t = 0.127$  mm, The two side walls both have cross-sectional dimensions  $2a = 2.54$  mm and  $a+t = 1.397$  mm and the substrate has cross-sectional dimensions  $6a = 7.62$  mm,  $a = 1.27$  mm and  $\epsilon_r = 2.56$ . Figure 11 compares the

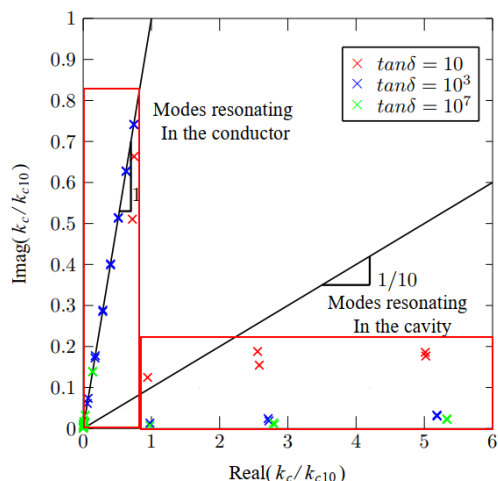


**Figure7:** Normalized complex cut off wave number for rectangular waveguide partially filled with PEC.

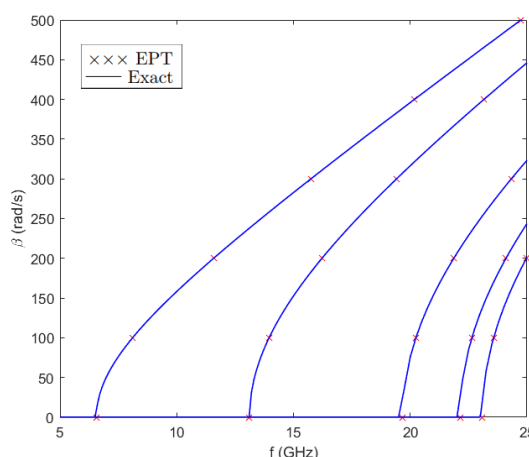


**Figure8:** Dispersion curve of a partially filled waveguide with  $a = 22.86$  mm,  $b = 10.16$  mm and  $d = 3.38$  mm.

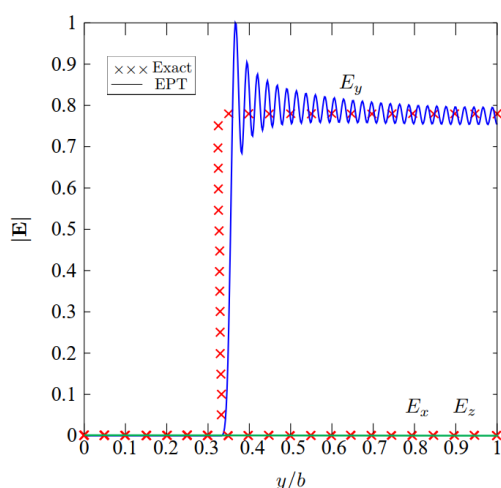


**Figure9:** Electric field distribution for the dominant mode for a partially filled waveguide with  $a= 22.86$  mm,  $b = 10.16$  mm, and  $d = 3.38$  mm.

**Table 2:**Numbering scheme of the modes used to generate results in Figures 7, 8 and 9.

	$n_x$	$n_y$
Solenoidal TE	0,1	j
Solenoidal TM	1	j
Irrotational	1	j
Limits	$0 \leq j \leq 20$	

dispersion relation obtained using EPT with the numbering scheme of modes as shown in Table 3 and those obtained using the commercial solver HFSS. It is clear that excellent agreement is achieved for the different propagating modes.

Third, shielded coplanar waveguide problem is illustrated in Figure 12. The case to be considered is of a line which has cross-sectional dimensions  $A = 12.7$  mm and  $B = 12.7$  mm, The patch has cross-sectional dimensions  $a = 1.27$  mm and  $t = 0.127$  mm, The two side walls both have cross-sectional dimensions  $4a = 5.08$  mm and  $a+t = 1.397$  mm and the substrate has cross-sectional dimensions  $2a = 2.54$  mm,  $a = 1.27$  mm and  $\epsilon_r = 2.56$ . Figure 13 compares the dispersion relation obtained using EPT with the numbering scheme of modes as shown in Table 4 and those obtained using the commercial solver HFSS. It is clear that excellent agreement is achieved for the different propagating modes.

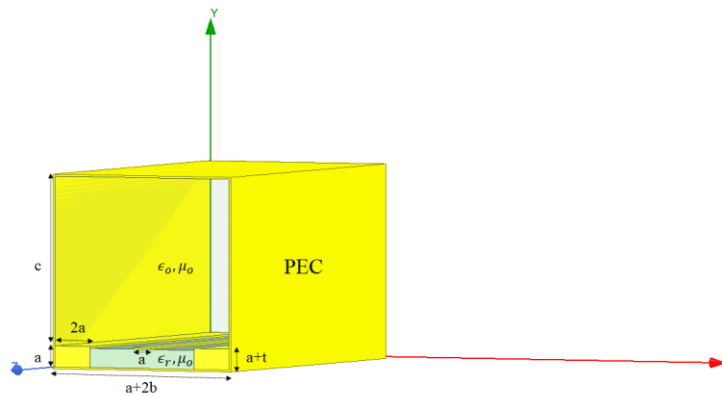


**Figure10:** Shielded microstrip transmission line.

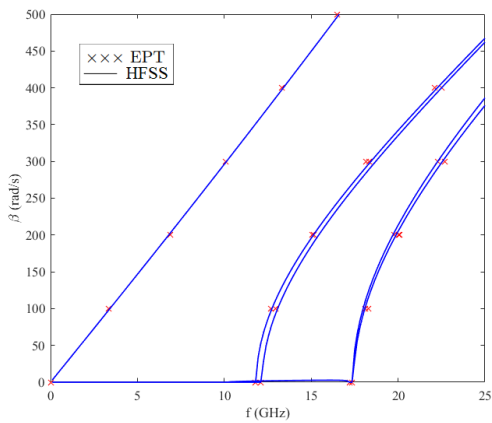


**Figure11:** Dispersion curve of shielded microstrip transmission line.

**Table 3:**Numbering scheme of the modes used to generate results in Figure 11.

	$n_x$	$n_y$
Solenoidal TE	i	j
Solenoidal TM	i	j
Irrotational	i	j
Limits	$0 \leq i \leq 25$ $0 \leq j \leq 35$	

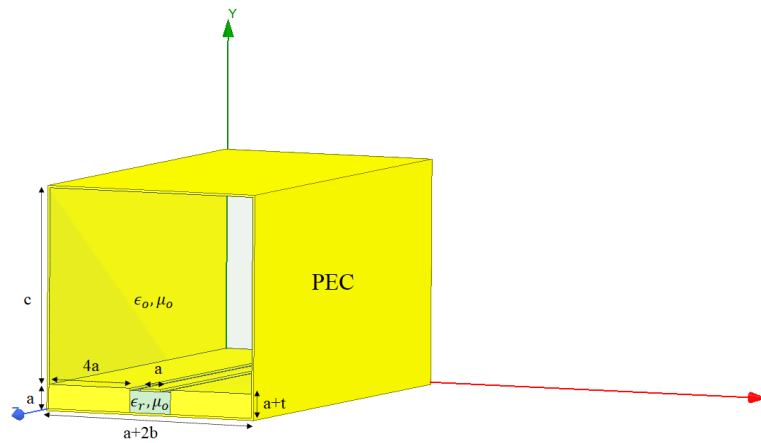


**Figure12:** Shielded coplanar waveguide.



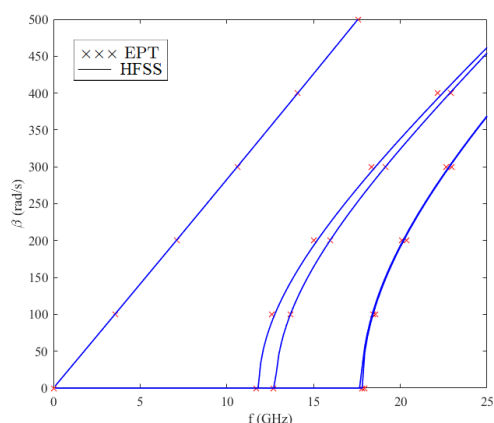


**Figure13:** Dispersion curve of shielded microstrip transmission line.

**Table 4:**Numbering scheme of the modes used to generate results in Figure 13.

	$n_x$	$n_y$
Solenoidal TE	i	j
Solenoidal TM	i	j
Irrotational	i	j
Limits	$0 \leq i \leq 30$ $0 \leq j \leq 35$	

#### IV. Conclusion

Throughout this work, an eigenmode projection technique was utilized to solve the problems of the electromagnetic wave propagation in shielded transmission lines. The technique is adopted to solve the problems of infinite length rectangular shaped loaded lines. The EPT was shown to have many advantages compared to other conventional numerical techniques where it provides an automatic selection for the basis functions using complete orthogonal functions. It doesn't require an explicit subwavelength segmentation for the structure prior to the solution flow. The involved integrals have no singularity issues, and their kernels are typically sinusoidal for rectangular canonical structures. The integrals are also frequency independent, which means that all integrals will be calculated only one time through the solution flow to obtain the dispersion curve. Integrals are linear with permittivity, which allows for scaling of the integrals in case of the presence of the variable dielectric constants.

#### References

- [1]. L. Rayleigh, "On the passage of electric waves through tubes," *Philosophical Magazine*, vol. 43, 1897.
- [2]. K. S. Packard, "The origin of waveguides: A case of multiple rediscovery," *IEEE Transactions on Microwave Theory and Techniques*, MTT-32, Sep. 1984.
- [3]. D. M. Pozar, "Microwave engineering," in, 4th ed. John Wiley and Sons, Inc., 2012, ch. 3.
- [4]. C. A. Balanis, *Advanced Engineering Electromagnetics*. John Wiley and Sons, Inc., 2012.
- [5]. R. M. Barrett, "Microwave printed circuits a historical survey," *IRE Trans. Microwave Theory Tech.*, MTT-3, Mar. 1955.
- [6]. W. J. Getsinger, "Microstrip dispersion model," *IEEE Trans. Microwave Theory Tech.*, MTT-22, Jan. 1973.
- [7]. A. Wexler, "Solution of waveguide discontinuities by modal analysis," *Microwave Theory and Techniques, IEEE Transactions*, vol. 15, no. 9, pp. 508–517, Sep. 1967.
- [8]. R. H. MacPhie and K.-L. Wu, "A plane wave expansion of spherical wave functions for modal analysis of guided wave structures and scatterers," *IEEE Transactions on Antennas and Propagation*, vol. 51, no. 10, pp. 2801–2805, 2003.
- [9]. F. Moglie, T. Rozzi, P. Marcozzi, and A. Schiavoni, "A new termination condition for the application of fdtd techniques to discontinuity problems in close homogeneous waveguide," *IEEE Microwave and Guided Wave Letters*, vol. 2, no. 12, pp. 475–477, 1992.
- [10]. Z. Lou and J.-M. Jin, "An accurate waveguide port boundary condition for the time domain finite-element method," *IEEE transactions on microwave theory and techniques*, vol. 53, no. 9, pp. 3014–3023, 2005.
- [11]. A. Belenguer, H. Esteban, V. E. Boria, C. Bachiller, and J. V. Morro, "Hybrid mode matching and method of moments method for the full-wave analysis of arbitrarily shaped structures fed through canonical waveguides using only electric currents," *IEEE Transactions on Microwave Theory and Techniques*, vol. 58, no. 3, pp. 537–544, 2010.
- [12]. M. Othman, T. Abuelfadl, and I. Eshrah, "Analysis of microwave cavities using an eigenmode projection approach," *Antennas and Propagation Society International Symposium (APSURSI), 2012 IEEE*, pp. 1–2, 2012.
- [13]. M. Othman, I. Eshrah, and T. Abuelfadl, "Analysis of waveguide discontinuities using eigenmode expansion," *Microwave Symposium Digest (MTT), 2013 IEEE MTT-S International*, 2013.
- [14]. M. H. Nasr, I. A. Eshrah, and T. M. Abuelfadl, "Electromagnetic scattering from dielectric objects using the eigenmode projection technique," *IEEE Transactions on Antennas and Propagation*, vol. 62, no. 6, pp. 3222–3231, Jun. 2014.
- [15]. A. F. Abdel-Rahman and T. M. Abuelfadl, "Transient analysis of circular waveguide probe excitation using cavity modal expansion," *2015 IEEE International Symposium on Antennas and Propagation USNC/URSI National Radio Science Meeting*, pp. 1510–1511, Jul. 2015.
- [16]. M. H. Nasr, I. A. Eshrah, and T. M. Abuelfadl, "Electromagnetic scattering from dielectric objects using the eigenmode projection technique," *IEEE Transactions on Antennas and Propagation*, vol. 62, no. 6, pp. 3222–3231, Jun. 2014.
- [17]. J. C. Slater, *Microwave electronics*. D Van Nostrand Company, 1950, pp. 467–473.
- [18]. K. Kurokawa, "The expansions of electromagnetic fields in cavities," *IEEE Trans. Microwave Theory Techn.*, vol. 6, pp. 178–187, Apr. 1955.
- [19]. R. E. Collin, *Foundations for Microwave Engineering*. IEEE Press Series on Electromagnetic Wave Theory, Wiley-Interscience, 2001, pp. 525–540.

- [20]. J. G. V. Bladel, *Electromagnetic Fields*. IEEE Press Series on Electromagnetic Wave Theory, Wiley-Interscience, pp. 509-520, 2007.
- [21]. T. K. Mealy, I. A. Eshrah, and T. M. Abuelfadl, "Solution of periodically loaded waveguides using the eigenmode projection technique," in *Microwave Symposium (IMS), 2016 IEEE MTT-S International*, IEEE, 2016, pp. 1-4.

Mohamed O. Ashour, et. al. "Solution of Electromagnetic Propagation Problems in Shielded Transmission Lines Using the Eigenmode Projection Technique." *IOSR Journal of Electronics and Communication Engineering (IOSR-JECE)* 17(3), (2022): pp 39-48.